JACS
JOURNAL OF THE AMERICAN CHEMICAL SOCIETY
Communication
pubs.acs.org/JACS

Landing and Catalytic Characterization of Individual Nanoparticles on Electrode Surfaces

Steven E. F. Kleijn,[†,§] Stanley C. S. Lai,[‡,§] Thomas S. Miller,[‡] Alexei I. Yanson,[†] Marc T. M. Koper,*[,†] and Patrick R. Unwin*[,‡]

[†]Leiden Institute of Chemistry, Leiden University, P.O. Box 9502, 2300 RA Leiden, The Netherlands
[‡]Department of Chemistry, University of Warwick, Coventry CV4 7AL, United Kingdom

Supporting Information

ABSTRACT: We demonstrate a novel and versatile pipet-based approach to study the landing of individual nanoparticles (NPs) on various electrode materials without any need for encapsulation or fabrication of complex substrate electrode structures, providing great flexibility with respect to electrode materials. Because of the small electrode area defined by the pipet dimensions, the background current is low, allowing for the detection of minute current signals with good time resolution. This approach was used to characterize the potential-dependent activity of Au NPs and to measure the catalytic activity of a single NP on a TEM grid, combining electrochemical and physical characterization at the single NP level for the first time. Such measurements open up the possibility of studying the relation between the size, structure and activity of catalyst particles unambiguously.

Metal nanoparticles (NPs) have been extensively studied as electrocatalysts in numerous fields and applications.[1] A key aspect of NPs is their size- and structure-dependent reactivity,[1c] which is often inferred from "top-down" studies of ensembles of catalytic NPs. However, because of the inherent variance in NP size and shape, only average reactivity trends may be obtained in this way. Even when one can work with a narrow size distribution, subtle effects may substantially alter the reactivity. Indeed, we showed in a previous study that ostensibly similar NPs can have very different reactivities as a result of subtle variations in morphology.[2] Therefore, to truly understand NP reactivity on a fundamental level, it is imperative to study single NPs. While such an investigation is demanding, as it requires placing, locating, and characterizing a single NP, a few experimental studies of this type have been reported.[2,3] Single NP studies are further challenging because of the need for high-accuracy measurement of small (current) signals with reasonable bandwidth.[3h,4]

A recent innovative method for electrochemical detection of NPs[3a−f] focuses on NPs that are dispersed in an electrolyte solution and can diffuse to and land on an electrode surface held at a potential where a reaction occurs on the catalytic NP but not on the inert collector electrode. Consequently, the arrival of a NP at the electrode surface results in an increase in current due to the NP reaction, which can be a reaction of a species in solution[3a] or the oxidation of the NP itself.[3d] To limit the number of NPs that land and to minimize the background current, a collector electrode with a small area is needed. The preparation of such ultramicroelectrodes (UMEs) greatly limits the choice of substrate materials, since not every material (particularly materials of practical importance) can be shaped to micro- or nanoscale dimensions, and even when the material can be encapsulated, electrode preparation requires considerable time and effort.[5] A typical UME (~5 μm diameter) often still shows a considerable background signal compared with the electrochemical signal from the NP reaction.[3a−f] Consequently, only large current signals (often resulting from mass-transport-limited reactions)[3a,b] can be detected, and obtaining an entire current−voltage response at an individual NP has to date proved impossible. Furthermore, subsequent structural characterization of the immobilized NPs has proven to be very challenging.[5b]

In this paper, we demonstrate the study of the reactivity of single NPs by employing scanning electrochemical cell microscopy (SECCM) to select and isolate a small area on a collector electrode formed from any kind of material and to land, detect, and characterize individual NPs. The experimental setup is schematically depicted in Figure 1a,b and described in full in the Supporting Information (SI). In short, a dual-channel (theta)

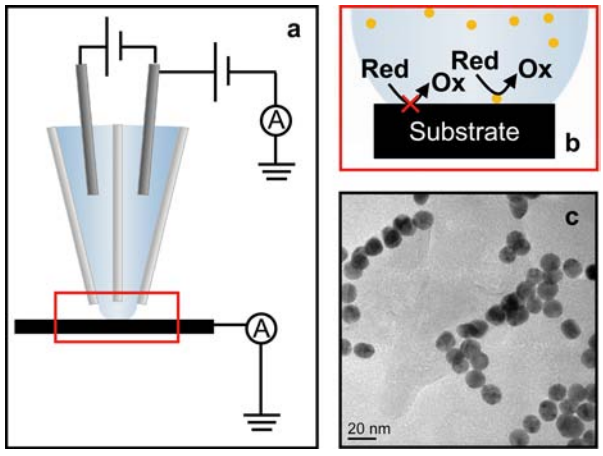

Figure 1. (a) Schematic of the experimental setup. (b) Schematic of the liquid meniscus that constitutes the electrochemical cell. The substrate is held at a potential where a reaction occurs on the catalytic AuNP but not on the collector electrode. (c) TEM image of the AuNPs used in this study.

Received: September 17, 2012
Published: October 26, 2012

   dx.doi.org/10.1021/ja309220m | J. Am. Chem. Soc. 2012, 134, 18558−18561

pipet with a sharp point having a diameter of ~1.5 μm was filled with an electrolyte solution of interest [containing ~70 pM citrate-capped gold NPs (AuNPs) with diameters of 10–20 nm;[6] Figure 1c] and two Pd–H_2 quasi-reference counter electrodes (QRCEs) [E^0 = 50 mV vs reversible hydrogen electrode (RHE)][2] held at the same potential. All potentials throughout this study are reported relative to the RHE. While in principle a single-barrel pipet could be used, the theta pipet allowed us to monitor the size of the liquid meniscus formed at the end of the pipet by measuring the ionic current between the two QRCEs across the meniscus when a small potential bias was applied, minimizing the variability between experiments. Furthermore, the migration rate of charged species could be controlled by the bias potential applied between the QRCEs,[7] although this option was not employed in the present work. The pipet was mounted on a piezoelectric positioning system and slowly lowered toward the substrate, which was held at ground, while the current flowing through the substrate was monitored continuously. Upon contact of the liquid meniscus at the end of the pipet with the substrate, a current spike due to the formation of the electrical double layer was observed at the substrate. This was used to halt the approach automatically, and the pipet was held in place for the duration of the experiment. The resulting meniscus between the pipet and substrate constitutes a micro- or nanoscopic electrochemical cell with the wetted area of the substrate as the working electrode, which experiences a potential of the same magnitude but opposite sign as the potential applied to the QRCEs. In this approach, we isolate an area on the working electrode by limiting the electrolyte contact (rather than by decreasing the size of the working electrode as in previous studies),[3a–f] which results in at least three main advantages. First, this allows the use of a wide range of electrode materials, sizes, and morphologies, as no traditional UME manufacture is required; instead the method relies on facile micro- or nanopipet preparation. Second, we can make and break the cell at will on a specific site on the electrode surface (on a millisecond time scale if needed) simply by moving the pipet toward or away from the substrate. This is particularly beneficial if one wishes to land single NPs in a predetermined pattern. Finally, the working electrode area in this pipet-based approach is determined by the size of the pipet,[7,8] which can be routinely prepared to be smaller than a typical UME (of several micrometers in diameter), down to <200 nm.[9] Such ultrasmall surface areas result in a significant decrease in background current (by 2 orders of magnitude) compared with the UMEs presently used, allowing detection of much smaller currents from the NP reaction itself.

To demonstrate the flexibility of the pipet-based approach, we landed AuNPs from an aerated 5 mM phosphate buffer solution (pH 7.2) on highly oriented pyrolytic graphite (HOPG) at various potentials. HOPG is an interesting substrate because it serves as a model for novel sp^2 carbon materials and there has been recent debate on the active sites for electron transfer.[8] Furthermore, the surface of HOPG is easily refreshed (through cleaving with adhesive tape) and has a low background current, making it an attractive collector electrode for NP landing experiments.

Typical current–time plots obtained for the landing of AuNPs on HOPG at various potentials (Figure 2a–d) show a few general trends. Initially, with the pipet suspended in air, the recorded substrate current was zero. Bringing the liquid meniscus into contact with the substrate closed the electronic circuit, leading to an initial current spike at all potentials (e.g., at ~90 s in Figure 2a). This current spike can be attributed to the formation

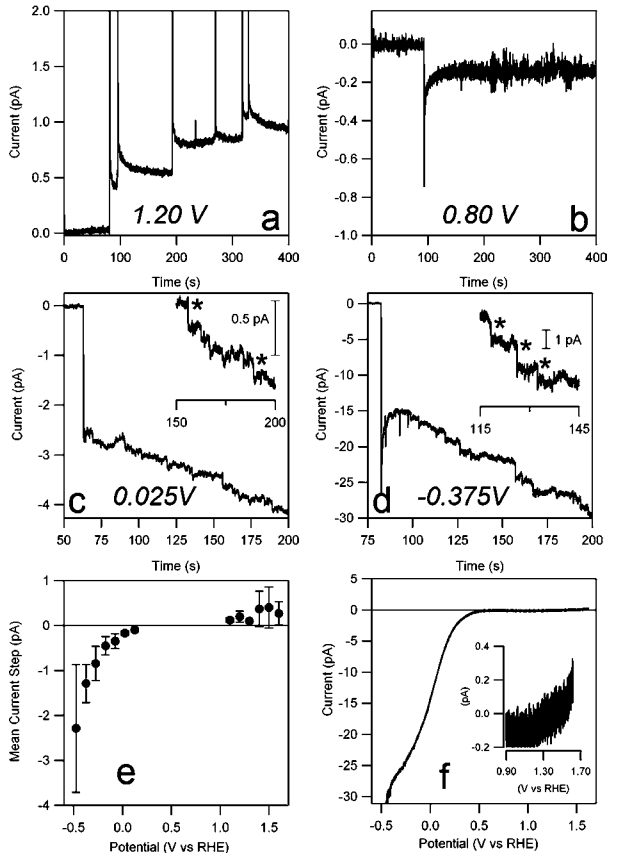

Figure 2. (a–d) Current–time plots showing the landing of the pipet meniscus (initial spike) and AuNPs (subsequent steps) at selected potentials. The current steps in the insets of (c) and (d) are marked (*). (e) Mean current step height determined as a function of substrate potential. Error bars denote 2σ. (f) Linear sweep voltammogram (50 mV s^{-1}) of Au in 5 mM phosphate buffer, measured using a pipet with a diameter of 1.5 μm.

of the electric double layer on the HOPG substrate, and its direction is indicative of the potential applied to the substrate relative to its potential of zero total charge (pztc). In view of the flexibility of this technique, this finding also opens up the possibility of quickly probing the pztc of a material at the nanoscale under various experimental conditions. When the meniscus was in contact with the substrate, discrete current steps were observed at potentials where electrochemical reactions could occur on Au but not on HOPG, indicating the arrival of distinct AuNPs. Three potential regimes can be distinguished: at potentials above 1 V (e.g., at 1.2 V in Figure 2a), the current steps were positive. At potentials below 0.15 V (Figure 2c,d), the current steps were negative, and the magnitude was larger at more cathodic potentials. Finally, at intermediate potentials (Figure 2b), no current steps were observed; instead, the current–time profile showed a constant background. To provide an understanding of this current–potential behavior in more detail, Figure 2e shows the mean value of the current steps as a function of substrate potential. There is a clear and strong potential dependence, similar to that of a bulk polycrystalline Au electrode measured using the same pipet setup (Figure 2f), although the current densities on the AuNPs were higher because of the much increased mass-transport rate at nanostructures in the SECCM setup.[9] At low potentials (<0.15 V), the observed current steps can be ascribed to the oxygen reduction reaction (ORR). The onset potential appears to be at a higher

dx.doi.org/10.1021/ja309220m | J. Am. Chem. Soc. 2012, 134, 18558–18561

overpotential than on bulk Au (~0.4 V), but the apparent difference is likely due to the fact that the current steps at lower overpotential are not sufficiently large to be detected, although we also cannot rule out some kinetic effects at the smaller particle due to the greatly enhanced mass-transport rate. At intermediate potentials, in the double-layer region of Au, no current steps were observed, as no reaction took place on the AuNP upon landing. This also indicates that the landing of NPs did not disturb the HOPG double layer significantly, while the charging of the particles themselves was not detected. Finally, at potentials more positive than 1.10 V, oxidative current steps were observed. Typically, surface oxide formation takes place in this potential range. However, as this process would be limited by the Au surface area, it should lead to current spikes with a finite charge (~5 fC for a 20 nm diameter AuNP)[10] rather than current steps. As the oxidation of carbonaceous species is often found to take place in the Au surface oxidation region,[11] we tentatively attribute the oxidative current steps to the oxidation of residual carbonaceous species in solution, as no special effort was taken to purify the solution and reagents.

The excellent signal-to-noise ratio in these experiments allowed ready analysis of the frequency (number of current steps divided by the run time of an experiment) at which AuNPs land on the HOPG substrate as a function of the substrate potential (Figure 3). At the extreme potentials, the experimentally observed frequency was ~0.05 s^{-1}, which is lower than the theoretical value of 0.4 s^{-1} predicted by diffusion laws[12] (see the SI). Similar discrepancies have been consistently reported previously.[3c,d,13] Although various explanations have been forwarded to account for this discrepancy, the issue is not yet well understood. Finally, it should be noted that at moderately high potentials (between 1.0 and 1.5 V), the observed landing frequency was below the average frequency. As the magnitude of the current steps was very small in this potential region, we ascribe the diminished observed frequency to the fact that only particularly large or active particles show a catalytic response large enough to be detected, and thus, the observed frequency may not represent the "true" landing frequency.

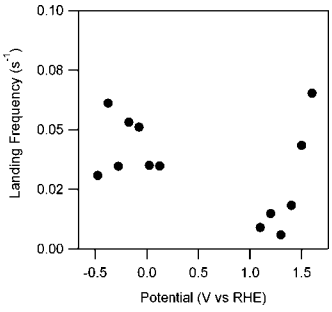

Figure 3. Frequency of current steps for landed NPs measured at different potentials.

A particularly exciting substrate on which to perform NP landing experiments is a transmission electron microscopy (TEM) grid, as this allows characterization of the deposited NPs to resolve fully the structure–activity relationships at the single NP level. To demonstrate this capability, we landed AuNPs on a carbon-coated TEM grid by measuring the oxidation of 2 mM hydrazine in a 50 mM citrate buffer. Although employing hydrazine with citrate-capped NPs gave rise to some complications (see below), it was a good model system for an electrocatalytic reaction, as it is sufficiently facile to reach mass-transport-limited conditions. Typical landing events with the TEM grid held at 1.25 V (a potential close to the mass-transport-limited regime) are shown in Figure 4a. As can be seen, in these experiments, establishing the contact of the meniscus with the carbon film on the TEM grid typically coincided with the landing of the first AuNP, giving rise to current steps of 40–80 pA. The magnitudes of these steps are in good agreement with predicted values of the diffusion-limited current i_{lim} based on radial diffusion to a sphere with radius r on a plane, as given by eq 1,[3a]

$$i_{lim} = 4\pi(\ln 2)nFDCr \quad (1)$$

where n is the number of electrons transferred per hydrazine molecule (4), F is the Faraday constant (9.649×10^4 C mol^{-1}), C is the hydrazine concentration (2 μmol cm^{-3}), and D is the diffusion coefficient of hydrazine. A wide range of D values for hydrazine have been reported, typically $(0.5–1.5) \times 10^{-5}$ cm^2 s^{-1}.[14] In this case, we found the best correspondence between the spread in the current step magnitudes and the AuNP size distribution using $D \approx 1.2 \times 10^{-5}$ cm^2 s^{-1}, a value well within the reported range and typical for small molecules.

The landing frequency was low, with up to tens of seconds between successive landing events. This is attributable to a much lower concentration of free AuNPs in solution due to extensive aggregation.[13] This aggregation was observed qualitatively upon addition of small amounts of hydrazine of a fairly concentrated AuNP solution by the color change from pink to gray followed by AuNP precipitation. Occasionally, these aggregates blocked the pipet completely, and no landings could be observed. In other cases, as Figure 4 shows, it was still possible to land single AuNPs

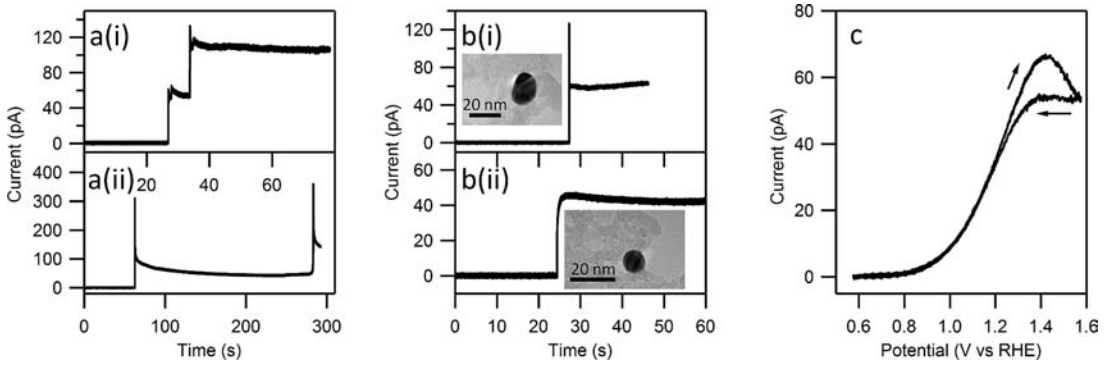

Figure 4. (a) Landing of AuNPs on a carbon-coated Cu TEM grid held at 1.25 V in the presence of 2 mM N_2H_4. (b) Landing events of individual AuNPs, with the *same* AuNP imaged by TEM afterward. (c) CV (200 mV s^{-1}) measured for the individual AuNP (i) shown in (b).

dx.doi.org/10.1021/ja309220m | *J. Am. Chem. Soc.* 2012, 134, 18558–18561

without interference from the landing of aggregates, possibly because the aggregates remained mobile in solution; in such cases, the opening at the end of each barrel of the pipet (~700 nm) may act as a particle size filter. Furthermore, we cannot exclude other effects, such as local interactions of the substrate with the AuNPs or the electrolyte solution, that may have contributed to the lower landing frequency relative to the HOPG substrate. Regardless, the long period between events allowed electrochemical characterization of each AuNP and then retraction of the pipet, leaving the initial AuNP on the TEM grid for subsequent visualization without additional AuNP landings. This allowed us to correlate the electrochemical response (current) with the physical properties of the AuNP. Examples are shown in Figure 4b: two separate landing experiments were performed with current steps of 40 and 60 pA. Visualization of these *same* particles with TEM showed that this difference was directly related to the difference in the sizes of the two AuNPs, with the current steps of 40 and 60 pA originating from NPs with diameters of ~10 and ~15 nm, respectively, in good agreement with eq 1. This agreement directly indicates that mass transport controls the reactivity of single AuNPs at this potential, and, moreover, the scaling of the current with particle radius confirms that the mass transport to a single particle is predominantly radial in nature.

Finally, we were able to sweep the substrate potential after the initial landing event to record a full cyclic voltammogram (CV) of a single AuNP before retracting the pipet. The CV recorded for the AuNP in Figure 4b(i) showed an onset potential of ~0.8 V (Figure 4c), in good agreement with those reported for hydrazine oxidation on gold electrodes.[15] The oxidation wave was somewhat drawn out compared with those in CVs recorded on macroscopic Au electrodes,[15] which can be fully ascribed to the increased mass-transport coefficient in this configuration (~6 cm s^{-1}; cf. ~10^{-3} cm s^{-1} for macroscopic systems).[8]

In conclusion, we have demonstrated a SECCM-based approach for landing and characterizing single NPs on electrodes with minimal electrode preparation and the ability to select the measurement location. The results obtained with this approach are consistent with previous NP landing studies on UMEs,[3a−f] but exhibit enhanced sensitivity due to the lower background signals resulting from the smaller contact area. As highlighted herein, this pipet-based approach eliminates the need for UME fabrication, and a wide variety of substrates can be investigated. A particularly exciting application was the use of this pipet-based approach to study NP reactivity on a TEM grid, which allowed a complete, unambiguous correlation of physical and electrochemical properties at the single NP level for the first time. Apart from studying particle size and shape effects, the wide range of substrates that can be studied also opens up the possibility of studying substrate effects in electrocatalytic reactions, an aspect which is not yet well understood. We believe that these prospects make this pipet-based approach particularly powerful for further understanding and resolving nanoparticle reactivity.

■ ASSOCIATED CONTENT

Supporting Information

Experimental setup, materials, AuNP synthesis, and calculation of the expected landing frequency. This material is available free of charge via the Internet at http://pubs.acs.org.

■ AUTHOR INFORMATION

Corresponding Author

m.koper@chem.leidenuniv.nl; p.r.unwin@warwick.ac.uk

Author Contributions

[§]S.E.F.K. and S.C.S.L. contributed equally.

Notes

The authors declare no competing financial interest.

■ ACKNOWLEDGMENTS

We gratefully acknowledge Dr. Alex Colburn and Mr. Kim McKelvey for useful discussions and instrumentation design and development. This work was supported by a Marie Curie Intra European Fellowship within the Seventh Framework Programme of the European Community (275450 "VISELCAT") to S.C.S.L., a European Research Council Advanced Investigator Grant (ERC-2009-AdG 247143 "QUANTIF") to P.R.U., and The Netherlands Organisation for Scientific Research (NWO) through VIDI and VICI Grants awarded to A.I.Y. and M.T.M.K., respectively.

■ REFERENCES

(1) (a) Somorjai, G. A. *Science* **1985**, *227*, 902. (b) Koper, M. T. M. *Nanoscale* **2011**, *3*, 2054. (c) Chen, A.; Holt-Hindle, P. *Chem. Rev.* **2010**, *110*, 3767.

(2) Lai, S. C. S.; Dudin, P. V.; Macpherson, J. V.; Unwin, P. R. *J. Am. Chem. Soc.* **2011**, *133*, 10744.

(3) (a) Xiao, X. Y.; Bard, A. J. *J. Am. Chem. Soc.* **2007**, *129*, 9610. (b) Bard, A. J.; Zhou, H.; Kwon, S. J. *Isr. J. Chem.* **2010**, *50*, 267. (c) Xiao, X.; Fan, F.-R. F.; Zhou, J.; Bard, A. J. *J. Am. Chem. Soc.* **2008**, *130*, 16669. (d) Zhou, Y.-G.; Rees, N. V.; Compton, R. G. *Angew. Chem., Int. Ed.* **2011**, *50*, 4219. (e) Rees, N. V.; Zhou, Y.-G.; Compton, R. G. *RSC Adv.* **2012**, *2*, 379. (f) Kwon, S. J.; Bard, A. J. *J. Am. Chem. Soc.* **2012**, *134*, 7102. (g) Meier, J.; Friedrich, K. A.; Stimming, U. *Faraday Discuss.* **2002**, *121*, 365. (h) Chen, S.; Kucernak, A. *J. Phys. Chem. B* **2003**, *107*, 8392. (i) Krapf, D.; Wu, M.-Y.; Smeets, R. M. M.; Zandbergen, H. W.; Dekker, C.; Lemay, S. G. *Nano Lett.* **2005**, *6*, 105.

(4) (a) Eikerling, M.; Meier, J.; Stimming, U. *Z. Phys. Chem.* **2003**, *217*, 395. (b) Hoeben, F. J. M.; Meijer, F. S.; Dekker, C.; Albracht, S. P. J.; Heering, H. A.; Lemay, S. G. *ACS Nano* **2008**, *2*, 2497.

(5) (a) Kleijn, S. E. F.; Yanson, A. I.; Koper, M. T. M. *J. Electroanal. Chem.* **2012**, *666*, 19. (b) Li, Y. X.; Cox, J. T.; Zhang, B. *J. Am. Chem. Soc.* **2010**, *132*, 3047. (c) Cox, J. T.; Zhang, B. *Annu. Rev. Anal. Chem.* **2012**, *5*, 253.

(6) (a) Frens, G. *Nat. Phys. Sci.* **1973**, *241*, 20. (b) Turkevich, J.; Stevenson, P. C.; Hillier, J. *Discuss. Faraday Soc.* **1951**, *11*, 55.

(7) Snowden, M. E.; Güell, A. G.; Lai, S. C. S.; McKelvey, K.; Ebejer, N.; O'Connell, M. A.; Colburn, A. W.; Unwin, P. R. *Anal. Chem.* **2012**, *84*, 2483.

(8) Lai, S. C. S.; Patel, A. N.; McKelvey, K.; Unwin, P. R. *Angew. Chem., Int. Ed.* **2012**, *51*, 5405.

(9) Güell, A. G.; Ebejer, N.; Snowden, M. E.; McKelvey, K.; Macpherson, J. V.; Unwin, P. R. *Proc. Natl. Acad. Sci. U.S.A.* **2012**, *109*, 11487.

(10) Angerstein-Kozlowska, H.; Conway, B. E.; Barnett, B.; Mozota, J. *J. Electroanal. Chem.* **1979**, *100*, 417.

(11) Lai, S. C. S.; Kleijn, S. E. F.; Öztürk, F. T. Z.; Vellinga, V. C. V.; Koning, J.; Rodriguez, P.; Koper, M. T. M. *Catal. Today* **2010**, *154*, 92.

(12) Bard, A. J.; Faulkner, L. R. *Electrochemical Methods: Fundamentals and Applications*, 2nd ed.; Wiley: New York, 2001.

(13) Kleijn, S. E. F.; Serrano-Bou, B.; Yanson, A. I.; Koper, M. T. M. Submitted for publication.

(14) (a) Zare, H. R.; Nasirizadeh, N. *Electrochim. Acta* **2007**, *52*, 4153. (b) Raoof, J.-B.; Ojani, R.; Mohammadpour, Z. *Int. J. Electrochem. Sci.* **2010**, *5*, 177. (c) Karp, S.; Meites, L. *J. Am. Chem. Soc.* **1962**, *84*, 906.

(15) Alvarez-Ruiz, B.; Gomez, R.; Orts, J. M.; Feliu, J. M. *J. Electrochem. Soc.* **2002**, *149*, D35.